Optimal Operation of a Plug-in Hybrid Vehicle with Battery Thermal and Degradation Model

Jongho Kim[1,*] Youngsuk Park[1] John D. Fox[2] Stephen P. Boyd[1] William Dally[3]

Abstract— **We propose a control method to optimally use fuel and battery resources for the power-split plug-in hybrid vehicles (PHEVs) under the predetermined driving route and associated energy demand profile. We integrate both battery thermal model and degradation model and formulate a mixed-integer convex problem which can be approximately solved with standard efficient solvers. In experiment, we demonstrate that our controller can balance battery usage to avoid severe battery degradation and fuel usage optimally, depending on ambient temperature or energy demand profiles of the routes. Under various scenarios, the results are validated by the Autonomie software [1] and compared with conventional existing CDCS controller and the earlier related work [2], which only optimize to achieve minimal fuel use and neglect battery degradation. Lastly, we show the superiority of our controller fast enough to be computed on the on-board vehicle computer and applied in real-time.**

I. INTRODUCTION

A. Motivation

Development of Electric vehicles (EVs), hybrid and plug-in hybrid vehicles (PHEVs) is an active research area for next-generation vehicles. Heywood et al. [3] suggest that market share of hybrid and PHEVs is estimated to reach 30% by 2050 and emphasize both growing demands and the promising future of EVs and PHEVs. PHEVs in particular have drawn many attentions in recent vehicle developments since they have controllers which are capable of shifting energy resources to the electricity grid rather than only using petroleum sourced energy. Recent studies [4][5][6] have shown that the choice of internal energy resource during the route can have substantial impacts on the overall vehicle efficiency. The operation of the vehicle battery, and scheduling the resource use during a trip, are interesting control problems.

In PHEVs, the main stored energy component except the fuel resource is the battery and the most prevalent battery type is the Lithium ion (Li-ion). Li-ion type batteries are attractive for their high power density and longer cycle life compared to other battery types [7]. Because of the growing interest on Li-ion type batteries for EVs and PHEVs, several researchers [8][9][10] have investigated operational properties of these batteries and highlighted the importance of understanding Li-ion battery degradation. The degradation of a battery is a complex electrochemical phenomenon and some researchers propose degradation models and present validation via extensive empirical-based results from experimental laboratory tests. However, most models are presented in non-formulated forms. For example, Wang et al.[11] states that for current less than half of the absolute value of current rate (*i.e.*, $C/2$), battery degradation does not depend on current and propose a corresponding model. On the other hand, Zabala et al. [9] propose a model which defines the input current as a main dependent variable.

Many PHEV controllers implement strategies without extensively considering the resulting battery degradation. A simple and most common strategy in PHEVs is Charge-Depletion Charge Sustaining (CDCS) controller which starts a trip with a near fully-charged battery and runs on the electric drive until the battery is discharged to a certain threshold. After this point on a trip, the vehicle uses the fuel resources and engine to operate as a traditional hybrid, charging the battery and maintaining a nominal charge level in operation. All of this CDCS, other controller including table-based or empirical control models, and the earlier work [2] are naive in a sense that they do not consider the battery degradation effect and/or the efficient balancing of both the ICE and the battery during trips.

This paper is focused on finding the control strategy which simultaneously optimizes the battery degradation and fuel resource usage based on the prior knowledge of the route energy demand profile. We assume that the prior route information is fully determined. This prior information could be from well-trained statistical estimation models of prior routes or accurate GPS data measurements, which can be separate research topic and thus is out of our focus in this paper. Although this assumption is not always true in reality, the techniques from this paper are still generally applicable along with efficient route prediction methods. We use convex optimization to obtain the efficient optimal control strategy.

B. Contributions

We summarize our contributions as follows:

- Consider the problem that minimize the fuel efficiency and battery degradation of PHEVs with vehicle dynamic constraints, integrating battery thermal and degradation model into optimal control problem.
- Propose tractable formulation via convex relaxation, transforming the non-convex terms into reasonable convex ones.
- Validate via experiments that our method can manage to suffer less battery degradation than that of other controller including CDCS and the controller on our earlier related work [2].

[*]Corresponding author
[1]Department of Electrical Engineering, Stanford USA.
[2]Department of Applied Physics, Stanford USA.
[3]Department of Computer Science, Stanford USA.

C. Outline

We structure the paper in the following way. The general backgrounds for power-split PHEV and battery model is introduced in Section 2. In Section 3, we use convex optimization to formulate the optimal control problem under pre-determined route profile. In Section 4, we compare our optimal controller to other existing controller including CDCS and validate the results.

II. Background

We explain our hybrid vehicle model, battery models. We consider the time horizon $[0,T]$ where T denotes the time of arrival (*i.e.*, end of a trip). The required vehicle speed is assumed to be known based on precise route estimation models and the desired drive power $P_{\mathrm{drv}}(t) \in \mathbf{R}$ over the route can be obtained accordingly.

A. Drivetrain

We consider the power-split PHEV which can be found in cars such as Toyota Prius. This kind of drivetrain uses two on-board energy sources which are fuel, $P_{\mathrm{fuel}}(t) \in \mathbf{R}$ and battery $P_b(t) \in \mathbf{R}$. The drivetrain combines these available powers to output the drive power $P_{\mathrm{drv}}(t) \in \mathbf{R}$. We denote $P_b(t) > 0$ as power extracted from the battery source and $P_b(t) < 0$ as power returned to the source. Battery energy has a limited amount of power, *i.e.*,

$$p_b^{\min} \le P_b(t) \le P_b^{\max} \tag{1}$$

and the fuel does not return energy so $P_{\mathrm{fuel}}(t) \ge 0$ for all $t \in [0,T]$.

The drivetrain model has a converter which allows to switch between two different discrete modes. We denote $\theta(t) \in \{0,1\}$ as the mode at time t. $\theta(t) = 0$ represents engine-off in which all the power comes from the battery only and for $\theta(t) = 1$, the drive power is a function of P_{fuel} and P_b. In other words,

$$P_{\mathrm{drv}}(t) = \begin{cases} P_b(t) & \text{if } \theta(t) = 0 \\ f(P_{\mathrm{fuel}}(t), P_b(t)) & \text{if } \theta(t) = 1 \end{cases} \tag{2}$$

We assume the function $f : \mathbf{R} \times \mathbf{R} \mapsto \mathbf{R}$ is increasing in each argument and *concave*. Although this assumption is not always guaranteed, it is true for all cases we have examined. f is often not known in closed form but we can represent P_{fuel} as a function of P_{b} and P_{drv} since f is increasing in each argument, *i.e.*,

$$P_{\mathrm{fuel}}(t) = h(P_b(t), P_{\mathrm{drv}}).$$

For detailed definitions and explanations, please refer to our previous paper [2] and justification therein.

a) Engine: The amount of combustion fuel power consumed is given by hF, where $h \in \mathbf{R}$ is the (constant) heating value of the fuel and $F \in \mathbf{R}$ is the total fuel quantity used. Denoting the fuel price as $\pi \in \mathbf{R}$, we define the total cost of fuel used as

$$J_{\mathrm{fuel}} = (\pi h) \int_0^T P_{\mathrm{fuel}}(t) dt. \tag{3}$$

B. Battery

There are many possible equivalent circuit models describing battery dynamics and in this work we use a very simple RC equivalent circuit. The battery model is RC finite reservoir with a finite total energy capacity of 7.8 kWh, a nominal voltage $V \in \mathbf{R}$ and internal resistance $R_{\mathrm{int}} \in \mathbf{R}$.

a) Battery Powerloss: Battery losses are determined as P^2 loss term which penalizes large withdrawals of battery power in short amounts of time. In our model, if we require a certain amount power P_e to run the motors, the power P_b withdrawn from the battery is

$$P_b = \left(P_e + \tfrac{1}{2} P_e^2 \tfrac{R_{\mathrm{int}}}{V^2}\right) / P_{\mathrm{eff}} \tag{4}$$

where $P_{\mathrm{eff}} \in \mathbf{R}$ is the efficiency of the power converters. The analogous expression is used for expressing losses while charging the battery.

b) Battery energy: Given an initial battery energy

$$\dot{E}_b(0) = E_b^{\mathrm{init}} \tag{5}$$

with $E_b^{\mathrm{init}} \in \mathbf{R}$, the energy is drawn from battery is

$$\dot{E}_b(t) = -P_b(t) \tag{6}$$

c) Battery Thermal Model: Battery temperature during operation may greatly affect performances, life and reliability of the battery system. The heat generation in the batteries are from two major sources: 1) electrochemical operation and 2) Joule heating. Thermal modeling of battery relies heavily on the fundamental of heat transfer [12]. Deriving a perfectly precise model for heat transfer is challenging due to the complexity of battery chemistry and material compositions [13]. In this work, we adopt a simple heat transfer model as follows

$$mC \tfrac{dT_b}{dt} = |P_b| + h_{\mathrm{trans}} (T_b - T_{\mathrm{amb}}) \tag{7}$$

Here, $m \in \mathbf{R}$ is the total mass of battery, $C \in \mathbf{R}$ is the heat capacity of battery, $h_{\mathrm{trans}} \in \mathbf{R}$ is heat transfer coefficient, $T_{\mathrm{amb}} \in \mathbf{R}$ is ambient temperature and $T_b \in \mathbf{R}$ is the battery temperature at time t. Note that C depends on composition and chemistry of batteries and h_{trans} may also reflect the efficiency of battery cooling system in PHEVs. (Refer to Table I for specifications to adopt in Appendix.) We set the initial battery temperature as the ambient temperature, *i.e.*, $T_b(0) = T_{\mathrm{amb}}$.

d) Battery Degradation Model: Battery degradation is caused by the structural and chemical transformations such as electrolyte oxidation at the cathode and growth of solid electrolyte interface on the anode [14]. Two kinds of battery degradation effects have been studied in literature [7], [11], [9] as follows: 1) calendar aging (without using battery) and 2) cyclic aging (using battery). Calendar aging is dependent on temperature and state-of-charge (SOC) which are coupled with an Arrhenius relationship which results in an underlying dependency on time (t^z) where z tends to be $1/2$. Cycling aging is dependent on temperature, charge/discharge current and total charge/discharge delivered which is often referred as *Ah throughput*. Here, we regard cyclic aging as main degradation affected by the optimal controller and focus on it. Let $Q_d(t) \in \mathbf{R}$ be the cumulative degradation or loss of capacity so far and $\dot{Q}_d(t) \in \mathbf{R}$ be the battery degradation rate at time t. The following simple degradation model on PHEV battery has been suggested by Ahmadian et al. [13]

$$\dot{Q}_d(t) = c_1 \exp\left(\frac{c_2 + c_3|I_b(t)|}{R_{\text{gas}} T_b}\right) \cdot g(\mathbf{I_b}(t)) \tag{8}$$

where c_1, c_2, $c_3 \in \mathbf{R}_+$ are fitted constants varied by the types of battery, $R_{\text{gas}} = 8.314$ $[J \cdot \text{mol} \cdot K^{-1}]$ is gas constant, and $I_b(t) \in \mathbf{R}$ is charging/discharging battery current (*i.e.*, $P_b(t) = I_b^2(t) R_{\text{int}}$. For discretized current $\mathbf{I_b}(t) = \{I_b(0), \ldots, I_b(t)\}$ with time interval Δt, we define $g(\cdot)$ as the difference of total charge delivered

$$g(\mathbf{I_b}(t)) = \left(\left(\sum_{\tau=0}^{t} |I_b(\tau)|\right)^z - \left(\sum_{\tau=0}^{t-1} |I_b(\tau)|\right)^z \right) / \Delta t.$$

with $z = 0.5$.

This model expresses the degradation effect with respect to charging rates and battery temperature. More specifically, the model is able to capture the following degradation properties: 1) the rate of degradation is faster under high $|I_b(t)|$ (or C-rate), 2) the model follows Arrhenius rule of the chemical activity on temperature, *i.e.*, chemical reaction is faster under high temperature $T_b(t)$ and high current $I_b(t)$, 3) the speed of degradation depends on cumulative charge of battery delivered over time.

e) Internal Resistance of Battery: Gong et al. [10] showed the dependency of battery internal resistance on battery SOC and different temperatures. Particularly, under the fixed temperatrue, the internal resistance R_{int} is almost constant within 20% to 80% battery SOC range (Refer to Figure 3.11 [10]). The value depends on battery temperature with Arrenhius model but the value stays within approximately 1 mΩ to 3 mΩ within moderate range of temperature.

III. Optimal Control

Our goal is to efficiently operate the drivetrain to meet the target power requirement $P_{\text{drv}}(t)$ for time t over the finite time horizon $[0, T]$. Here, we propose a formulation using convex relaxations that lead to a mixed-integer convex problem.

A. Constraints

a) Battery Temperature: EVs and PHEVs have preferable range of battery temperatures controlled by cooling systems because temperatures outside the desired range may severely affect the battery performances [15]. We have a finite capacity cooling system which regulates the battery temperature within a specific range of temperatures. Mathematically, we control the power dissipation in the battery to keep the battery temperature within

$$T^{\min} \leq T_b(t) \leq T^{\max} \tag{9}$$

over the horizon $[0, T]$. We set the minimum temperature to be ambient (*i.e.*, $T^{\min} = T_{\text{amb}}$) and allow maximum temperature to be $45°C$ above the ambient temperature of $25°C$ (*i.e.*, 343 K).

b) Finite Battery Resource: The battery energy has limits

$$E^{\min} \leq E(t) \leq E^{\max} \tag{10}$$

for all $t \in [0, T]$. In other words, the controller only allows the operation within a fixed range of the battery SOC. This constraint is common to prevent a severe battery degradation and usually $E^{\min}$ is 20% and $E^{\max}$ is 80% of the total battery energy.

B. Cost Function

The problem is to minimize four objectives including fuel cost (3) and here we specify each of them.

a) Switch Cost: We would like to minimize the number of times the engine turned on. Therefore, we introduce a switching cost $S \in [0, \infty]$ which is the number of times $\theta(t)$ switches on over the horizon $[0, T]$.

b) Cooling Cost: In our vehicle model, we choose a simple cooling system and define the cost of power usage by battery cooling system as

$$J_{\text{cooling}} = \int_0^T h_{\text{trans}} \left(T_b(t) - T_{\text{amb}}\right) dt. \tag{11}$$

This represents a passive cooling system which aims to set battery temperature to ambient temperature.

c) Degradation Cost: The cost of battery degradation is

$$J_{\text{degrad}} = \int_0^T \phi\left(\dot{Q}_d(t)\right) dt. \tag{12}$$

where $\phi : \mathbf{R} \mapsto \mathbf{R}$ is a non-negative and increasing cost function associated with the battery degradation rate.

d) Combination: Our total cost function for operating the vehicle is

$$J = J_{\text{fuel}} + \lambda_1 J_{\text{cooling}} + \lambda_2 J_{\text{degrad}} + \lambda_3 S \tag{13}$$

where λ_1, λ_2, $\lambda_3 \geq 0$. Note that our cost function depends on weight parameters (λ_1, λ_2 and λ_3) and the degradation cost function is depend on battery temperature T_b and battery power P_b.

C. Non-convex Problem

Therefore, the optimization problem is

$$\begin{array}{ll}
\text{minimize} & J := J_{\text{fuel}} + \lambda_1 J_{\text{cooling}} + \lambda_2 J_{\text{degrad}} + \lambda_3 S \\
\text{subject to} & P_{\text{fuel}}(t) = h_\theta(P_b(t), P_{\text{drv}}(t)) \\
& \dot{E}(t) = -P_b(t) \\
& P_b^{\min} \leq P_b(t) \leq P_b^{\max} \\
& E^{\min} \leq E(t) \leq E^{\max} \\
& E(0) = E^{\text{init}} \\
& T_b(0) = T_{\text{amb}} \\
& T^{\min} \preceq T_b(t) \preceq T^{\max} \\
& mC\dot{T}_b(t) = |P_b(t)| - h_{\text{trans}}\left(T_b(t) - T_{\text{amb}}\right),
\end{array} \tag{14}$$

with $t \in [0, T]$. This is a mixed integer non-convex optimization problem. There is no known efficient methods to find the global solution for this problem class.

D. Tractable Mixed-Integer Convex Problem via Relaxation

To solve (14) approximately, we convert it into the following mixed-integer convex problem.

$$
\begin{array}{ll}
\text{minimize} & J := J_{\text{fuel}} + \lambda_1 J_{\text{cooling}} + \lambda_2 \mathbf{J}_{\text{degrad}}^{\{\alpha\}} + \lambda_3 S \\
\text{subject to} & P_{\text{fuel}}(t) = h_\theta(P_b(t), P_{\text{drv}}(t)) \\
& \dot{E}(t) = -P_b(t) \\
& P_b^{\min} \leq P_b(t) \leq P_b^{\max} \\
& E^{\min} \leq E(t) \leq E^{\max} \\
& E(0) = E^{\text{init}} \\
& T_b(0) = T_{\text{amb}} \\
& T^{\min} \preceq T_b(t) \preceq T^{\max} \\
& \mathbf{mC\dot{T}_b(t)} \geq |\mathbf{P_b(t)}| - \mathbf{h}_{\text{trans}}\left(\mathbf{T_b(t)} - \mathbf{T}_{\text{amb}}\right),
\end{array}
\tag{15}
$$

with $t \in [0, T]$. Now we explain how to relax non-convex terms in (14) to (bold) convex ones above.

a) Relaxation on thermal model: Re-arranging the equation (7), we have

$$\dot{T}_b(t) = \left(|P_b(t)| - h_{\text{trans}}\left(T_b(t) - T_{\text{amb}}\right)\right)/mC.$$

Note that this is a non-affine equality constraint because the right hand side is a convex function for all $T_b \in \mathbf{R}$ and $P_b \in \mathbf{R}$. Since all equality constraints in convex optimization problem must be affine [16], we replace the constraint with

$$\dot{T}_b(t) \geq \left(|P_b(t)| - h_{\text{trans}}\left(T_b(t) - T_{\text{amb}}\right)\right)/mC. \tag{16}$$

This is a relaxation because not all solutions to (16) satisfies (7). However, it can be shown that this relaxation does not change the optimal solution set as long as the battery temperature is above ambient temperature from moderate usage of battery (or from temperature constraint).

b) Relaxation on degradation model: For degradation model, we assume the internal resistance to be constant $R_{\text{int}} = 2.5\ \text{m}\Omega$ within 20% to 80% SOC range and under moderate range of temperature (See Section II B-e). With simple assumption, we derive tractable convex surrogate cost function $J_{\text{degrad}}^{\{\alpha\}}$ using Least Square with fitting parameters $\{\alpha\} = (\alpha_1, \alpha_2, \alpha_3)$ as

$$J_{\text{degrad}}^{\{\alpha\}} = \int_{t=0}^{T} \left(\alpha_1 P_b^\tau(t) + \alpha_2 T_b^\tau(t) + \alpha_3 \int_{t'=0}^{t} P_b^\tau(t')dt'\right) dt. \tag{17}$$

See the details on how to fit over data in Appendix.

c) Efficient Computation: Using these approximations, the problem transforms to a mixed-integer convex optimization which can find the global solution using standard methods such as branch-and-bound and interior point method [16].

IV. Results and Analysis

A. Experiment Setting

a) Simulator: The model in Section 3 is a simplified model which can be run in real time. The optimal controller takes the simulated data and produces optimal strategy based on simplified model. To test the results from optimal controller, we use Autonomie, a simulator built by Argonne National Laboratory which has been studied and verified against various kinds of vehicles [1]. Since our work focuses on a PHEV model with two modes, we consider a vehicle which has specifications close to that of Toyota Prius. For detailed parameters of our vehicle and the cooling system, refer to our previous work [2] and Table I.

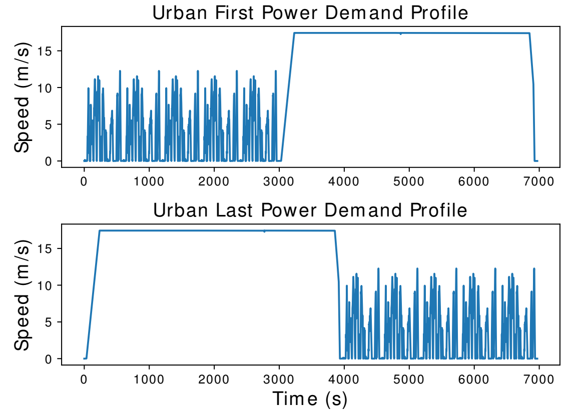

Fig. 1: Two power domain profile (P_{drv}) examples, consisting of an urban region and a suburban cruise region but with order interchanged. Cruise region requires constant medium speed of 39 mph (17.5 m/s).

b) Routes with Power Demand: We use six synthetic routes to test the efficiency of controllers where each route consists two different regions: one represents highway region with constant speed cruise and the other represents an urban region with numerous start-stop cycles and speed variations including zero. Routes have three different speed cruises: 1) medium speed (39 mph), 2) medfast speed (65 mph) and 3) fast speed (85 mph). Figure 1 represents two different routes with medium speed cruise component but inverted the order of the suburban and urban regions.

In our earlier related work [2], we observed that even though the total power demand is same for the mixed urban-suburban routes with order interchanged, the amount of fuel consumption varies depending on the control strategy employed by PHEVs. Here, we extend this observation to include battery degradation and see how battery thermal model and degradation model affects strategies of the optimal controller over various routes.

c) Weight Parameters: The objective of our optimization problem (15) is formed by the weighted sum of four objectives. Weights λ_1, λ_2 and λ_3 quantifies the importance of J_{cooling}, J_{degrad} and S respectively. Since our focus is on degradation model rather than power usage of cooling system, we set $\lambda_1 = 1$ for all cases. Also, we set $\lambda_3 = 20{,}000$ to encourage realistic total number of engine on/off switching. While fixing other weight parameters, we tune the parameter λ_2 to test our controller with appropriate battery degradation considerations. The value of J_{degrad} is not comparable to other objectives so it is important to adjust λ_2 to achieve efficient control strategy. For more sophisticated approach, we can incorporate λ_2 which reflects real economic cost ratio between fuel price and battery price, but here we use a simpler approach and defer to the longer version of our paper. For an effective hyper-parameter search, we normalize degradation parameters $\{\alpha\}$ (multiplying $\alpha_1+\alpha_2+\alpha_3$ to λ_2). Also, we test the effect of λ_2 by solving the problem (15) under different choices of λ_2.

d) Different Ambient Temperatures: The battery degradation model (17) depends on battery temperature T_b and it is mainly controlled by the cooling system (11) which aims to keep the T_b based on ambient temperature setting. Therefore, we test the effect of various ambient temperature settings under fixed weight parameters of our optimal controller. The temperature is ranging from 298K to 320K which represents the room temperature to relatively hot temperature.

e) Baselines: We compare our optimal controller with two baselines: CDCS controller and the controller on our earlier related work [2]. CDCS uses a simple strategy which preferentially uses battery first and then uses the fuel resources and engine for operation. The other controller aims to minimize the total fuel usage and the number of drivetrain switching modes. We simulate the synthetic routes under these three controllers and compare the performances.

B. Analysis

a) Balancing Resources and Battery Degradation over Different Routes: We tested our optimal controller on six different synthetic routes with known power demand profiles and compared it to two baselines. Figure 2 shows the battery SOC and combustion fuel use over time for a route with an urban region first and then suburban region with a medium speed cruise. Although all controllers starts and ends with same battery SOC, fuel consumption varies over the same route. The main difference is in the cruise component (approximately from time 3200 seconds) where our controller shows steady but smaller usage of battery energy compared to other controllers. As expected, optimal control without degradation shows significantly less fuel consumption compared with other two controllers while it also results in the most battery degradation as Figure 3 suggests.

Overall our optimal controller showed less degradation compared to other controllers over the routes we tested (Figure 4). The result is based on driving each route at exactly once and on average, our controller obtains 12% less battery degradation than that of CDCS. Also, our controller is able to maintain 17.5% more battery capacity than that of the other baseline controller. Based on these results, we can estimate how much the battery capacity (or life) would degrade after three years, assuming this trip is daily. Our controller is estimated to suffer battery capacity degradation about 16% at most while other two baselines suffer 20% or more battery capacity loss (See Figure 9 and 10 in Appendix for the detailed comparisons). These results emphasize that the control method is capable of balancing the efficiency between fuel and battery resources.

b) The Effect of Degradation Weight Parameters: Figure 5 shows the result on a route consisting urban region first and then suburban region with medium speed cruise. It

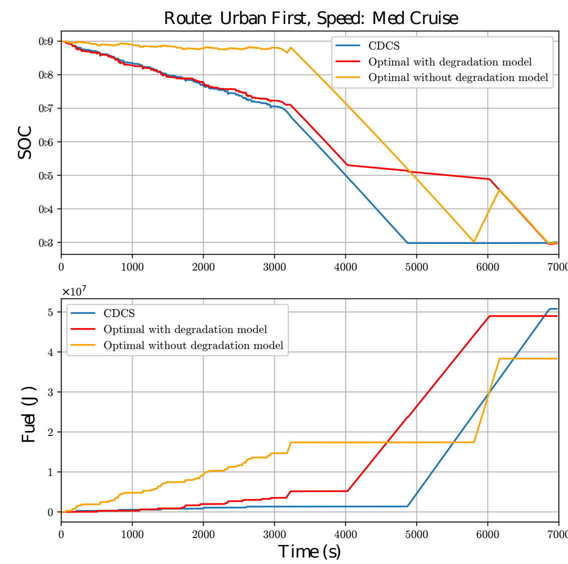

Fig. 2: Comparison of SOC and total fuel use of our controller (red) and baselines (blue, orange) after one cycle.

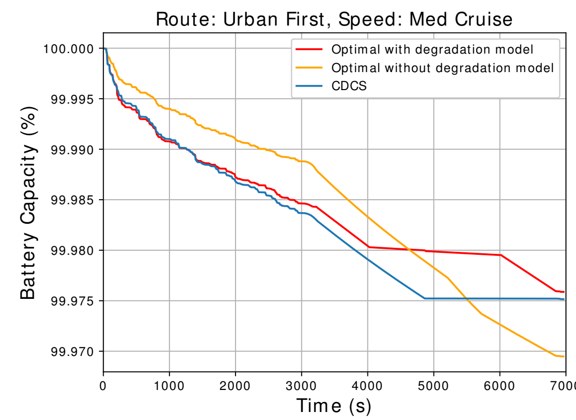

Fig. 3: Comparison of battery capacities remained over our controller (red) and baselines (blue, orange) after one cycle.

shows that increasing λ_2 weight encourages the controller to use more fuel while discourages battery usage.

c) The Operation on Various Ambient Temperature: Under fixed λ_1, λ_2 and λ_3, we tested various ambient temperatures, ranging from 298K (*i.e.*, ambient temperature) to 320K (*i.e.*, hot weather). Overall, higher ambient temperature resulted in more total fuel usage and less battery power (See Figure 6).

d) Computation: Most common other methods that attempt to solve optimal control problem for PHEVs is dynamic programming (DP) [17][18]. DP methods has been extensively studied both in theory and application but in general it requires a huge amount of computation power for PHEV applications. Our formulation (15) can be efficiently solved in Julia (and Convex.jl [19]) within a minute (on 2.6 GHz Intel Core i7 processor), which is fast enough to be computed in real time.

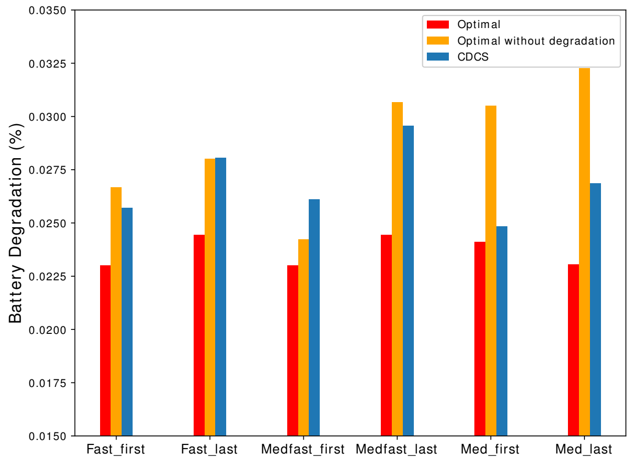

Fig. 4: Comparison of battery degradation, *i.e.*, Q_d, over six different routes after one drive cycle.

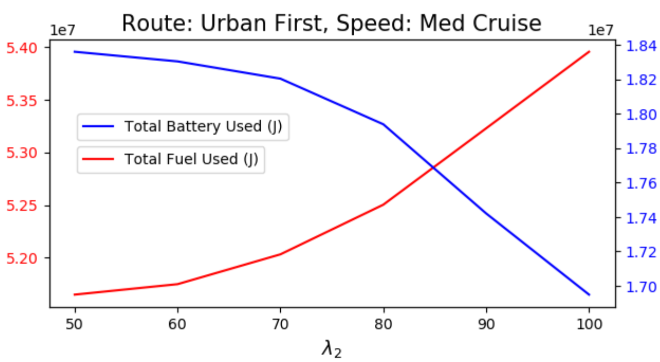

Fig. 5: The effect of using different λ_2 for the optimal control. As λ_2 increases, use fuel more and battery less.

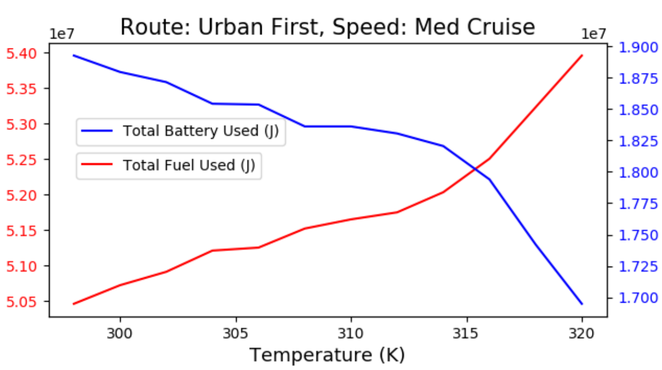

Fig. 6: The effect of different ambient temperature for the optimal control. In higher temperature, use battery less and fuel more instead.

V. Conclusion

We have proposed an efficient control method which balances the fuel and battery resources with taking battery degradation into consideration under the predetermined route and associated energy demand profile. To do so, we integrate a battery thermal model and battery degradation model into our problem, which extends the capability of the battery degradation control beyond that of CDCS or other controllers only designed to minimize fuel resources only. We posed a mixed-integer convex optimization problem and showed that our controller is capable of generating a tractable and efficient control strategy which is fast enough to be computed on the on-board vehicle computer.

This technique is readily applicable in current vehicles as well as future hybrid vehicles that manage fuel and battery resources during operation. Plugging in route estimation methods to the unknown route setting is an interesting discussion of future work. Another future extension for more practical purpose is developing the control method of power splitting over multiple resources more than two (beyond one fuel engine and one battery) over diverse real-world routes.

Acknowledgment

We would like to acknowledge contributions and support from J. Platt and N. Moehle. Many thanks to the Stanford-Ford Alliance program at Stanford University. We thank Dyche Anderson, Rajit Johri, Ming Kuang, Connie Qiu, Ming Cheng for useful discussion and feedback.

References

[1] Argonne National Laboratory, *Autonomie User Guide*, 2018.
[2] J. Platt, N. Moehle, J. D. Fox, and W. Dally, "Optimal operation of a plug-in hybrid vehicle," *IEEE Transactions on Vehicular Technology*, vol. 67, no. 11, pp. 10366–10377, 2018.
[3] J. Heywood and D. MacKenzie, "On the road toward 2050: Potential for substantial reductions in light-duty vehicle energy use and greenhouse gas emissions," tech. rep., MIT Energy Initiative Report, 2015.
[4] H. Helms, M. Pehnt, U. Lambrecht, and A. Liebich, "Electric vehicle and plug-in hybrid energy efficiency and life cycle emissions," *18th International Symposium Transport and Air Pollution*, 01 2010.
[5] I. Chung, H. Kang, J. Park, and J. Lee, "Fuel economy improvement analysis of hybrid electric vehicle," *International Journal of Automotive Technology*, vol. 20, pp. 531–537, Jun 2019.
[6] S. Moura, H. Fathy, D. Callaway, and J. Stein, "A stochastic optimal control approach for power management in plug-in hybrid electric vehicles," *Control Systems Technology, IEEE Transactions on*, vol. 19, pp. 545 – 555, 06 2011.
[7] H. Ibrahim, A. Ilinca, and J. Perron, "Energy storage systemscharacteristics and comparisons," *Renewable and Sustainable Energy Reviews*, pp. 1221–1250, 06 2008.
[8] A. Samba, "Battery electrical vehicles analysis of thermal modelling and thermal management," 2015.
[9] E. Sarasketa-Zabala, I. Gandiaga, L. Rodrguez-Martnez, and I. Villarreal, "Calendar ageing analysis of a lifepo4/graphite cell with dynamic model validations: Towards realistic lifetime predictions," *Journal of Power Sources*, vol. 272, p. 4557, 12 2014.
[10] X. Gong, "Modeling of lithium-ion battery considering temperature and aging uncertainties," in *Deep Blue*, University of Michigan-Dearborn, 2016.
[11] J. Wang, P. Liu, J. Hicks-Garner, E. Sherman, S. Soukiazian, M. Verbrugge, H. Tataria, J. Musser, and P. Finamore, "Cycle-life model for graphite-lifepo 4 cells," *Lancet*, vol. 196, pp. 3942–3948, 04 2011.
[12] N. H. F. Ismail, S. F. Toha, N. A. M. Azubir, N. H. M. Ishak, M. K. Hassan, and B. S. K. Ibrahim, "Simplified heat generation model for lithium ion battery used in electric vehicle," *IOP Conference Series: Materials Science and Engineering*, vol. 53, p. 012014, dec 2013.

[13] A. Ahmadian, M. Sedghi, A. Elkamel, M. Fowler, and M. Aliakbar Golkar, "Plug-in electric vehicle batteries degradation modeling for smart grid studies: Review, assessment and conceptual framework," *Renewable and Sustainable Energy Reviews*, 06 2017.

[14] "What causes li-ion to die?," *Battery University*, 2017.

[15] J. P. R., A. Pesaran, and K. Smith, "Electric vehicle battery thermal issues and thermal management techniques." SAE 2011 Symposium, 2011.

[16] S. Boyd and L. Vandenberghe, *Convex Optimization*. New York, NY, USA: Cambridge University Press, 2004.

[17] N. Denis, M. R. Dubois, J. P. F. Trovo, and A. Desrochers, "Power split strategy optimization of a plug-in parallel hybrid electric vehicle," *IEEE Transactions on Vehicular Technology*, vol. 67, pp. 315–326, Jan 2018.

[18] P. O'Keefe.M. and T. Markel, "Dynamic programming applied to investigate energy management strategies for a plug-in hev," 2006.

[19] M. Udell, K. Mohan, D. Zeng, J. Hong, S. Diamond, and S. Boyd, "Convex optimization in julia," in *Proceedings of the 1st First Workshop for High Performance Technical Computing in Dynamic Languages*, pp. 18–28, IEEE Press, 2014.

APPENDIX

A. Parameters

Parameters	Model
Battery mass	70.62 [Kg]
Heat capacity (C)	795 [J/ kg K]
h_{trans}	137.5 $[W/m^2K]$

TABLE I: Parameters for Battery Thermal Model

B. Upper Bound on Battery Degradation Model

Let $z = 0.5$. By Cauchy-Schwarz,

$$\sqrt{\sum_{\tau=0}^{t} |I_b(\tau)|} \leq \sqrt{\sum_{\tau=0}^{t-1} |I_b(\tau)|} + \sqrt{|I_b(t)|}.$$

Therefore, $g(\mathbf{I_b}(t)) \leq \sqrt{|I_b(t)|}$.

C. Least Square to Fit Degradation Cost

Note that $\sqrt{|P_b(t)|} \propto |I(t)|$ since the internal resistance, R_{int} is approximated by a constant, 2.5 mΩ. Now we use $P_b(t)$ as a variable in Q_d. First, we can set an upper bound on $g(\mathbf{I_b}(t))$ by $\sqrt{|I_b(t)|}$, i.e., $g(\mathbf{P_b}(t)) \leq P_b(t)^{\frac{1}{4}}$ and define $\phi(x) = \log(x+1)$, to obtain the following upper bound.

$$\log\left(\dot{Q}_d(t)+1\right) \leq \log(c_1) + \frac{c_2 + c_3|P_b(t)|}{R_{\text{gas}}T_b(t)} + \frac{1}{2}\log|P_b(t)|$$

where T_b and I_b are variables. The upper bound on right hand side is still not convex function because of I_b/T_b term as multiplying or dividing two variables does not guarantee convexity. In addition, the composite function $\log|\cdot|$ is not convex. Hence, this approximation is still not tractable with efficient convex optimization solver.

To achieve a tractable battery degradation model, we calculate Q_d based on our available route data $\tau \in \mathscr{D}$ and fit the model using least square method as follows

$$\min \sum_{\tau\in\mathscr{D}} \int_{t=0}^{T} \Big(\| \log(Q_d^{\tau}(t)+1) \\ - \alpha_1 P_b^{\tau}(t) - \alpha_2 T_b^{\tau}(t) - \alpha_3 \int_{t'=0}^{t} P_b^{\tau}(t')dt' \Big) dt \|_2^2 \tag{18}$$

with variables α_1, α_2 and $\alpha_3 \in \mathbf{R}$. Then, we obtain a tractable degradation cost function as

$$J_{\text{degrad}}^{\{\alpha\}} = \int_{t=0}^{T} \left(\alpha_1 P_b^{\tau}(t) + \alpha_2 T_b^{\tau}(t) + \alpha_3 \int_{t'=0}^{t} P_b^{\tau}(t')dt' \right) dt.$$

D. The results for different routes

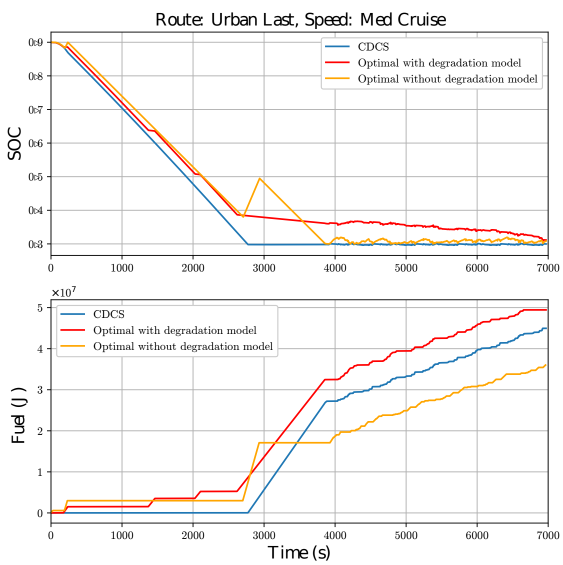

Fig. 7: Comparison of battery state-of-charge and total fuel use of our controller (red) and baselines (blue, orange). λ_2 is set to 70.

In some cases, our optimal controller generated a strategy with more fuel consumption than other controllers. For example, in Figure 7 and 8, our controller used significantly more fuel resources than those of two baselines. In this case, our controller decides to consume more fuel than battery resource to alleviate future battery degradation effects.

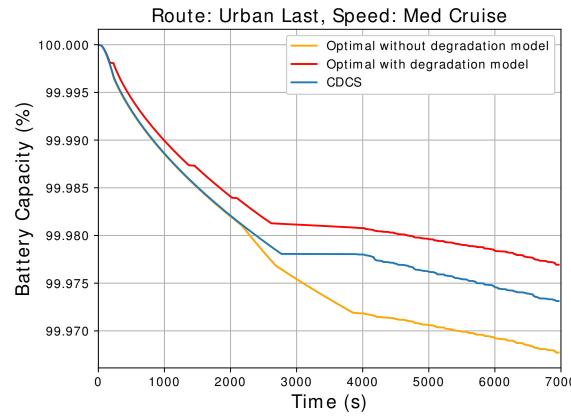

Fig. 8: Comparison of battery capacities remained over our controller (red) and baselines (blue, orange) after one cycle.

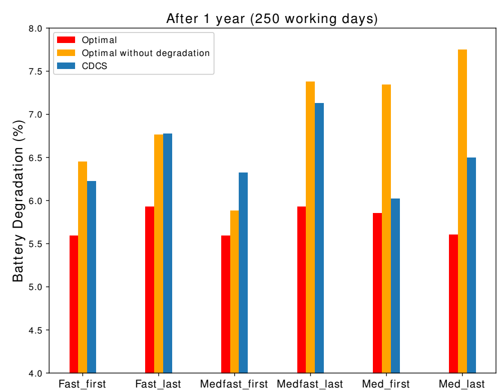

Fig. 9: Comparison of estimated battery degradation, i.e., Q_d, over six different routes for one year (250 route trips)

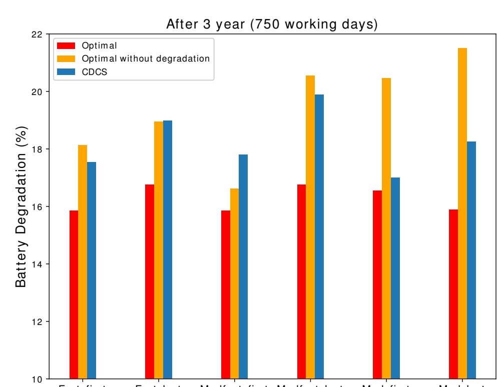

Fig. 10: Comparison of estimated battery degradation, *i.e.*, Q_d, over six different routes for three years (750 route trips)